Electrolytic Conversion of Bicarbonate Solutions to CO at >500 mA cm^{-2} and 2.2 V

Zishuai Zhang,[1] Eric W. Lees,[2] Shaoxuan Ren,[1] Aoxue Huang,[1] and Curtis P. Berlinguette*[1,2,3,4]

[1]Department of Chemistry, The University of British Columbia, 2036 Main Mall, Vancouver, British Columbia, V6T 1Z1, Canada.

[2]Department of Chemical and Biological Engineering, The University of British Columbia, 2360 East Mall, Vancouver, British Columbia, V6T 1Z3, Canada.

[3]Stewart Blusson Quantum Matter Institute, The University of British Columbia, 2355 East Mall, Vancouver, British Columbia, V6T 1Z4, Canada.

[4]Canadian Institute for Advanced Research (CIFAR), 661 University Avenue, Toronto, M5G 1M1, Ontario, Canada.

*Corresponding author: Curtis P. Berlinguette (cberling@chem.ubc.ca)

Abstract

Electrolyzers that reduce carbon dioxide (CO_2) into chemicals and fuels often use high-purity gaseous CO_2 feedstocks that need to be isolated from upstream carbon capture units. If CO_2 were to be captured directly from air, the eluent is likely to be an aqueous solution rich in bicarbonate ions (HCO_3^-). This scenario provides the impetus to electrolytically reduce these bicarbonate-rich carbon capture solutions into the same products as a CO_2 electrolyzer. We report here an electrolyzer configuration that couples the conversion of bicarbonate to CO at the cathode with hydrogen oxidation at an anode. This unique system is capable of reaching a commercially-relevant current density of 500 mA cm^{-2} at merely 2.2 V, which is >0.5 V more efficient than any other reported electrolyzer that reduces HCO_3^- or CO_2 at these current densities.

The CO_2 reduction reaction (CO2RR) is a means of using electricity to convert CO_2 into fuels and chemicals[1–4]. A commercial CO2RR electrolyzer will likely need to operate at current densities (J) greater than 200 mA cm^{-2} and cell voltages (V_{cell}) below 3 V[5–8]. The highest-performing CO2RR lab-scale electrolyzers are now capable of meeting these criteria when a pure gaseous CO_2 feedstock is used[9–14]. However, CO2RR electrolyzers must be effectively integrated with upstream carbon capture units (as well as downstream processes) to minimize capital and operational costs. A gaseous CO_2 feedstock will inevitably require CO_2 isolation and compression steps (Fig. 1)[15,16]. The isolation of CO_2 from air capture streams, for example, requires a series of reactions that require significant energy (e.g., 22.8 MJ to convert 100 mol of K_2CO_3 into CO_2; Fig. 1)[15]. The compression of CO_2 (2.0 MJ/100 mol CO_2) not only requires one-sixth the energy required for electrolysis (12.4 MJ/100 mol CO_2), but it also requires significant capital expenditures ($1–10 million USD/MW)[17]. Finally, electrolytic CO2RR produces OH$^-$, which reacts with >70% of consumed CO_2 to form unreactive (bi)carbonates (Eq. 1)[18–20]. Consequently, <20% of gaseous CO_2 is actually converted to product as it passes through the cathode compartment of a CO2RR electrolyzer (Fig. 1)[21].
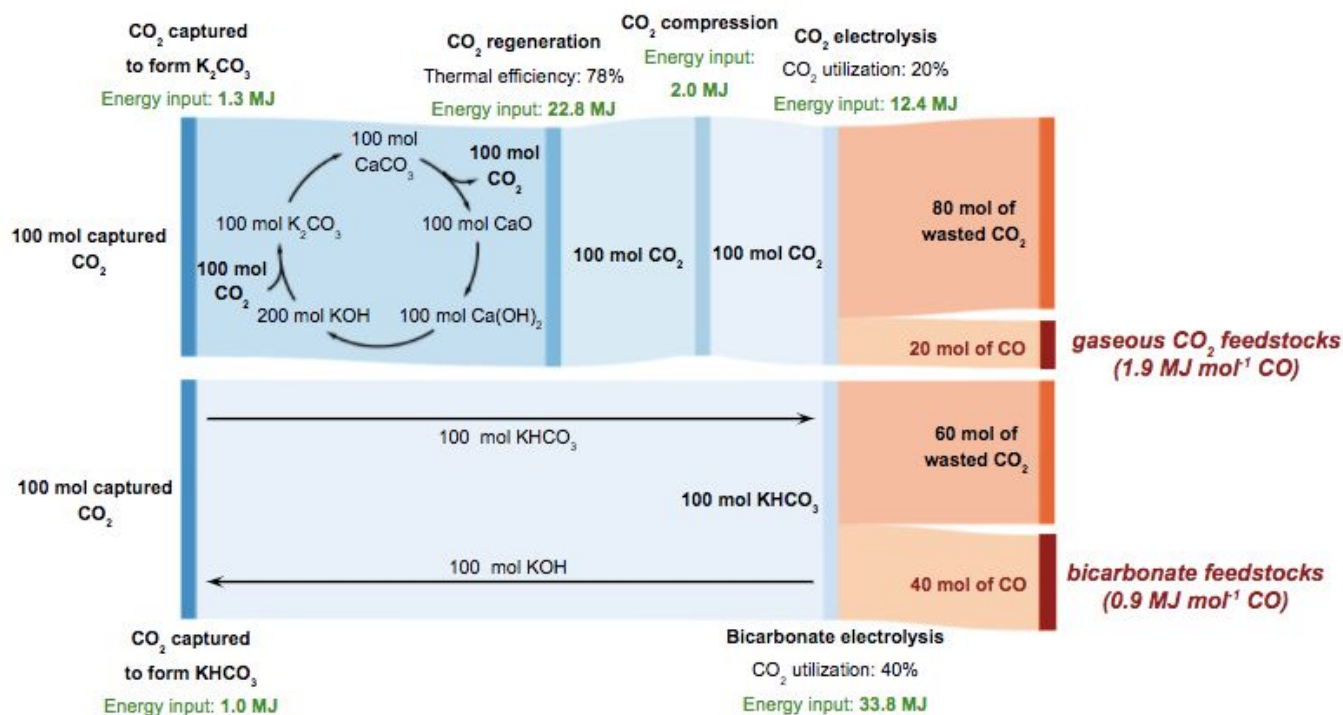
$$2OH^-_{(aq)} + CO_{2(g)} \rightleftharpoons CO_3^{2-}_{(aq)} + H_2O_{(l)} \qquad\qquad \text{Eq. 1}$$

Fig 1. Sankey diagrams illustrating CO_2 mass flows and energy inputs for the capture and conversion of atmospheric CO_2 into CO using electrolysis. The top diagram assumes captured CO_2 is regenerated using a direct air capture process[15,22], and that the electrolyzer is fed with a compressed $CO_{2(g)}$ feed (FE_{CO} = 90%; V_{cell} = 3.0 V; CO_2 utilization rate = 20%). The bottom panel relies on the electrolysis of $KHCO_3$, and bypasses the CO_2 regeneration and compression steps (FE_{CO} = 50%; V_{cell} = 2.2 V; CO_2 utilization rate = 40%). Energy inputs are sourced from Refs. 15, 22.

We sought to bypass these challenges by developing a CO2RR electrolyzer that uses a liquid bicarbonate feed instead of gaseous CO_2[23–26]. The efficient electrolysis of bicarbonate solutions (e.g., $KHCO_{3(aq)}$), a common eluant of carbon capture units, can form the same CO2RR products as an electrolyzer fed with gaseous CO_2, but without the need for CO_2 regeneration and pressurization (Fig. 1)[22]. Bicarbonate electrolyzers are also proven to yield CO_2 utilization values (the fraction of the CO_2 feedstock that is converted into the desired product) >40%; these values are much higher than the 1-20% typically reported for gaseous CO_2-fed electrolyzers[21,24,27]. The Sankey diagram in Fig 1 illustrates how a bicarbonate electrolyzer with a CO_2 utilization value of 40% makes a carbon product with twice the energy efficiency per mole of captured CO_2 as a gaseous CO_2-fed electrolyzer operating with an

aggressive CO_2 utilization value of 20%. This analysis makes a compelling case for considering the electrolysis of bicarbonate solutions over CO_2 feedstocks.

All reports of bicarbonate electrolysis to date use bipolar membranes (BPMs)[23,24,26,28–30]. These BPMs deliver H^+ to the cathode and convert HCO_3^- into CO_2 (Eq. 2), which is then electrochemically reduced at the cathode[23,30]. A key challenge in using a BPM is that an applied voltage of >0.83 V is required to dissociate water into OH^- and H^+ (Eq. 3)[31]. This voltage penalty makes it challenging to design an electrolyzer capable of operating at an industrially-relevant voltage of <3 V at high rates of product formation (Figs. S1, S2)[20].

$$H^+_{(aq)} + HCO_3^-{}_{(aq)} \rightleftharpoons CO_{2(g)} + H_2O_{(l)} \qquad \text{Eq. 2}$$

$$H_2O_{(l)} \rightleftharpoons H^+_{(aq)} + OH^-_{(aq)} \qquad \text{Eq. 3}$$

A significant voltage is also required to drive the oxygen evolution reaction (OER) at the anode (Eq. 4). This reaction provides a source of protons for CO2RR at the cathode, but the efficiency of the electrolyzer is constrained by the OER accounting for 90% of the equilibrium cell potential. This voltage penalty is seemingly unnecessary because the dioxygen product has little economic value and is usually flared to the environment. One strategy for eliminating this energy penalty is to source protons for the CO2RR from oxidation reactions that are more thermodynamically favourable than the OER[32–35]. Consider, for example, that the standard half-cell potential (E^0) for the hydrogen oxidation reaction (HOR; Eq. 5) is merely 0.0 V vs. the reversible hydrogen electrode (RHE) (*c.f.* E^0 = +1.23 V vs. RHE for the OER). HOR is widely used at the anode of fuel cells, but there is little precedent for its use in CO2RR electrolyzers[36,37].

$$4OH^-{}_{(aq)} - 4e^- \rightarrow 2H_2O_{(l)} + O_{2(g)} \qquad \text{Eq. 4}$$

$$H_{2(g)} - 2e^- \rightarrow 2H^+_{(aq)} \qquad \text{Eq. 5}$$

We report here a CO2RR electrolyzer designed to mediate bicarbonate electrolysis at the cathode in tandem with hydrogen oxidation at the anode. This system, which contains a cation exchange membrane (Nafion) that separates the cathode and anode compartments, operates with unprecedented performance parameters: a V_{cell} of 2.2 V (1.4 V after resistance compensation) at a current density of 500 mA cm^{-2}, and at a CO_2 utilization value of >25%. The lowest voltage (without resistance compensation) previously reported in the literature is >2.8 V at 500 mA/cm^2 [9]. This electrolyzer is configured to use the HOR at the anode to form protons, which are then transported through a Nafion membrane to the cathode compartment for reaction with bicarbonate to form CO_2 (Fig. S1). The CO_2 is formed at an electrocatalyst surface, and is therefore positioned to be reduced to form CO2RR products such as CO.

The title "zero-gap" electrolyzer reported here (denoted "HOR|Nafion|HCO_3^-" to indicate the anode|membrane|cathode configuration) presses the anode and cathode tightly against opposite faces of a Nafion membrane (25 µm). Flowplates with serpentine channels were used to deliver humidified H_2 gas and 3 M $KHCO_3$ to the anode and cathode, respectively (Fig. 2a). The gas diffusion electrode (GDE) in the anode chamber consisted of Pt on carbon black, while a silver foam electrode was used in the cathode chamber. This electrolyzer was used to perform electrolysis experiments at applied current densities over a 100 to 1000 mA cm^{-2} range. Product formation rates of CO and H_2 from the cathode compartment along with V_{cell} (the full cell voltage measured across the anode and cathode) were recorded over the course of the electrolysis experiments.

Using this reactor architecture, an electrolysis experiment at an applied current density of 100 mA cm^{-2} yielded a V_{cell} of 1.7 V. This value represents the lowest V_{cell} ever reported for a zero-gap CO2RR membrane reactor. When the current density was held at 500 mA cm^{-2} for 1 h, the measured V_{cell} was held below 2.2 V for the duration of the experiment (Fig. S2), which also sets a new benchmark for CO2RR electrolysis (Figs. S3, S4). Importantly, the CO_2 utilization values were measured to be >25% at 500 mA cm^{-2}.

We benchmarked these V_{cell} values against those obtained with our previously reported bicarbonate electrolyzer. This control system ("OER|BPM|HCO$_3^-$") contains a bipolar membrane (instead of Nafion) and mediates OER at a nickel anode (instead of HOR at a platinum anode). In order to maintain a current density of 100 mA cm^{-2}, the control system required a V_{cell} of 4.4 V. This value is more than twice as high as our new electrolyzer that performs HOR at the anode. The V_{cell} of the control system spiked to 18 V at 500 mA cm^{-2}, whereas the V_{cell} of our new electrolyzer was only 2.2 V at the same current density (Fig. 2b). The voltage penalties for water dissociation and the OER render the V_{cell} of the control system impractical for industrially-relevant current densities (i.e., $J > 200$ mA cm^{-2}).
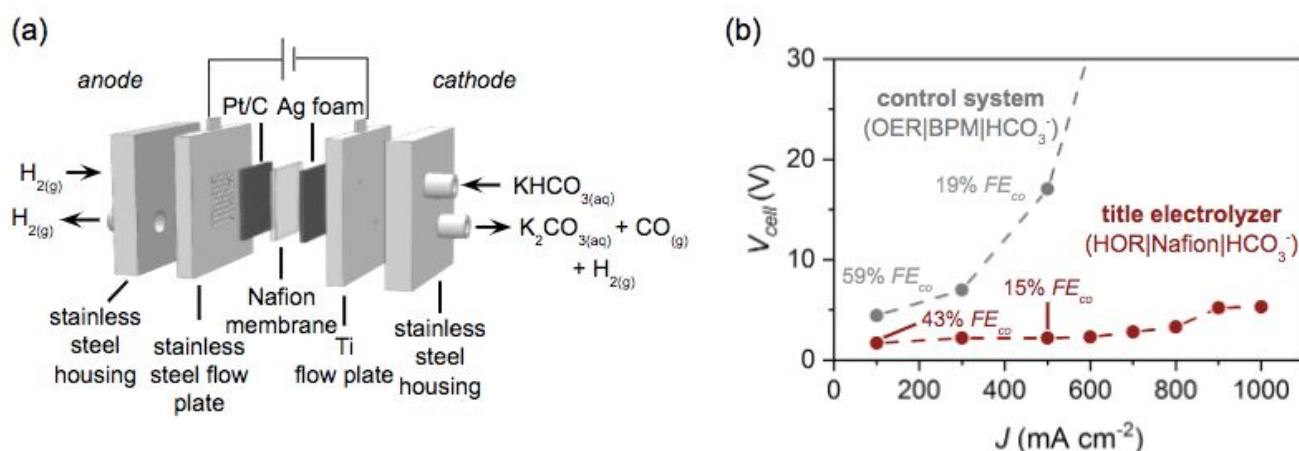

Fig 2. **The flow electrolyzer for efficient bicarbonate electrolysis with low full cell voltages.** (a) Schematic depiction of the title electrolyzer architecture with the anodic HOR and a Nafion membrane (25 μm). (b) V_{cell} values measured as a function of current density for the control system and the title electrolyzer with a Nafion membrane (25 μm).

While the V_{cell} and CO$_2$ utilization values from our electrolyzer that couples bicarbonate reduction and HOR are state-of-the-art, a major shortcoming of the system is that the measured faradaic efficiencies for CO production (FE_{CO}) were merely 43% at 100 mA cm^{-2} (15% at 500 mA cm^{-2}; Fig. 2b). We tested thicker Nafion membranes as a means of driving a higher proton flux through the membrane[27], but we did not observe any meaningful changes in FE_{CO} values for membrane thicknesses of 25 and 50 μm. However, we did observe higher FE_{CO} values upon integration of a 500-μm microfluidic buffer layer between the silver foam cathode and Nafion membrane (Fig. S5)[13,38]. This buffer layer serves to suppress

7

hydrogen evolution reaction (HER) by inhibiting H^+ transport from the membrane to the surface of the cathode (Eq. 5)[39]. Our experiments corroborated this effect, as the FE_{CO} increased from 47% to 71% at an applied current density 100 mA cm^{-2} with the thicker 50-μm membrane (Fig. S5). Notwithstanding, there is a substantial voltage penalty at high current densities when the buffer layer is used (Fig. S6). Electrocatalysts that favor CO2RR over HER in acidic media will be needed to increase FE_{CO}.

Another feature of our system is that the anode chamber is fed with H_2 gas instead of aqueous media (e.g., NaOH). Consequently, H_2 must be produced by the electrolysis of water or the steam-methane reformation (SMR) of natural gas. Our techno-economic analysis (TEA) shows that the title electrolyzer can produce CO profitably if the price of H_2 gas remains below $2.3/kg (Fig. S7, see Supplementary Materials for details), a value that is within the current price range of H_2 produced by SMR (i.e., $1.0-2.4/kg)[40–42]. Moreover, we calculate that bicarbonate electrolysis coupled with H_2 produced by SMR is carbon-negative if the H_2 utilization value is >32% (See Supplementary Materials for details). We expect H_2 utilization values >70% based on related hydrogen fuel cell studies[43,44]. There are also opportunities to couple our title electrolyzer to industrial processes (e.g., chlor-alkali process, chlorate production) where H_2 is generated as a waste by-product[40], and thus $H_{2(g)}$ could be provided at an even lower cost. Finally, we have also contemplated scenarios where $H_{2(g)}$ is recycled to further minimize the cost of using $H_{2(g)}$. Experiments shown in Fig. S8 shows that producing a liquid product (e.g., formate) enables $H_{2(g)}$ produced by HER to be recycled, thereby reducing the amount of virgin H_2 supplied to the system.

We demonstrate here an electrolyzer that mediates the conversion of bicarbonate into CO (or formate) at the CO_2 utilization values >25% at 500 mA cm^{-2}. By sourcing protons from the HOR instead of the OER, this electrolyzer requires merely 2.2 V to drive bicarbonate electrolysis at 500 mA cm^{-2}. Moreover, we show that the FE_{CO} of the electrolyzer can be increased to 71% at 100 mA cm^{-2} by integrating a 500-μm buffer layer between the silver foam cathode and Nafion membrane to slow the competitive HER. With these performance parameters, our TEA shows that this new electrolyzer can

produce CO economically at the market price for H_2 gas. These findings demonstrate a practical method for producing value-added carbon products from bicarbonate solutions with high energy efficiency.

References:

1. Weekes, D. M., Salvatore, D. A., Reyes, A., Huang, A. & Berlinguette, C. P. Electrolytic CO_2 Reduction in a Flow Cell. *Acc. Chem. Res.* **51**, 910–918 (2018).

2. Whipple, D. T. & Kenis, P. J. A. Prospects of CO_2 Utilization via Direct Heterogeneous Electrochemical Reduction. *J. Phys. Chem. Lett.* **1**, 3451–3458 (2010).

3. Hori, Y. Electrochemical CO_2 Reduction on Metal Electrodes. in *Modern Aspects of Electrochemistry* (eds. Vayenas, C. G., White, R. E. & Gamboa-Aldeco, M. E.) 89–189 (Springer New York, 2008).

4. Nitopi, S. *et al.* Progress and Perspectives of Electrochemical CO_2 Reduction on Copper in Aqueous Electrolyte. *Chem. Rev.* **119**, 7610–7672 (2019).

5. Salvatore, D. & Berlinguette, C. P. Voltage Matters When Reducing CO_2 in an Electrochemical Flow Cell. *ACS Energy Letters* **5**, 215–220 (2019).

6. Spurgeon, J. M. & Kumar, B. A comparative technoeconomic analysis of pathways for commercial electrochemical CO_2 reduction to liquid products. *Energy Environ. Sci.* **11**, 1536–1551 (2018).

7. Jouny, M., Luc, W. & Jiao, F. General Techno-Economic Analysis of CO_2 Electrolysis Systems. *Ind. Eng. Chem. Res.* **57**, 2165–2177 (2018).

8. De Luna, P. *et al.* What would it take for renewably powered electrosynthesis to displace petrochemical processes? *Science* **364**, eaav3506 (2019).

9. Arquer, F. P. G. de *et al.* CO_2 electrolysis to multicarbon products at activities greater than 1 A cm^{-2}. *Science* **367** 661–666 (2020).

10. Zhang, X. *et al.* Molecular engineering of dispersed nickel phthalocyanines on carbon nanotubes for selective CO_2 reduction. *Nature Energy* (2020) doi:10.1038/s41560-020-0667-9.

11. Chen, X. *et al.* Electrochemical CO_2-to-ethylene conversion on polyamine-incorporated Cu electrodes. *Nature Catalysis* (2020) doi:10.1038/s41929-020-00547-0.

12. Ren, S. *et al.* Molecular electrocatalysts can mediate fast, selective CO_2 reduction in a flow cell. *Science* **365**, 367–369 (2019).

13. Chen, Y. *et al.* A Robust, Scalable Platform for the Electrochemical Conversion of CO_2 to Formate: Identifying Pathways to Higher Energy Efficiencies. *ACS Energy Lett.* **5**, 1825–1833 (2020).

14. Endrődi, B. *et al.* High carbonate ion conductance of a robust PiperION membrane allows industrial current density and conversion in a zero-gap carbon dioxide electrolyzer cell. *Energy Environ. Sci.* **13**, 4098–4105 (2020).

15. Keith, D. W., Holmes, G., St. Angelo, D. & Heidel, K. A Process for Capturing CO_2 from the Atmosphere. *Joule* **2**, 1573–1594 (2018).

16. Smith, W. A., Burdyny, T., Vermaas, D. A. & Geerlings, H. Pathways to Industrial-Scale Fuel Out of Thin Air from CO_2 Electrolysis. *Joule* **3**, 1822–1834 (2019).

17. Luyben, W. L. Capital cost of compressors for conceptual design. *Chemical Engineering and Processing - Process Intensification* **126**, 206–209 (2018).

18. Larrazábal, G. O. *et al.* Analysis of Mass Flows and Membrane Cross-over in CO_2 Reduction at High Current Densities in an MEA-Type Electrolyzer. *ACS Appl. Mater. Interfaces* **11**, 41281–41288 (2019).

19. Ma, M. *et al.* Insights into the carbon balance for CO_2 electroreduction on Cu using gas diffusion electrode reactor designs. *Energy Environ. Sci.* **13**, 977–985 (2020).

20. Rabinowitz, J. A. & Kanan, M. W. The future of low-temperature carbon dioxide electrolysis depends on solving one basic problem. *Nat. Commun.* **11**, 5231 (2020).

21. Jeng, E. & Jiao, F. Investigation of CO_2 single-pass conversion in a flow electrolyzer. *Reaction Chemistry & Engineering* **5**, 1768–1775 (2020).

22. Welch, A. J., Dunn, E., DuChene, J. S. & Atwater, H. A. Bicarbonate or Carbonate Processes for Coupling Carbon Dioxide Capture and Electrochemical Conversion. *ACS Energy Letters* **5**, 940–945 (2020).

23. Li, T. *et al.* Electrolytic Conversion of Bicarbonate into CO in a Flow Cell. *Joule* **3**, 1487–1497 (2019).

24. Lees, E. W. *et al.* Electrodes Designed for Converting Bicarbonate into CO. *ACS Energy Letters* **5**, 2165–2173 (2020).

25. Zhang, Z. *et al.* pH Matters When Reducing CO_2 in an Electrochemical Flow Cell. *ACS Energy Lett.* **5**, 3101–3107 (2020).

26. Li, T., Lees, E. W., Zhang, Z. & Berlinguette, C. P. Conversion of Bicarbonate to Formate in an Electrochemical Flow Reactor. *ACS Energy Lett.* 2624–2630 (2020).

27. Ripatti, D. S., Veltman, T. R. & Kanan, M. W. Carbon Monoxide Gas Diffusion Electrolysis that Produces

Concentrated C2 Products with High Single-Pass Conversion. *Joule* **3**, 240–256 (2019).

28. Li, Y. C. *et al.* Electrolysis of CO_2 to Syngas in Bipolar Membrane-Based Electrochemical Cells. *ACS Energy Lett.* **1**, 1149–1153 (2016).

29. Zhang, Z. *et al.* Metallic Porous Electrodes Enable Efficient Bicarbonate Electrolysis. doi:10.26434/chemrxiv.12891071.v1.

30. Li, Y. C. *et al.* CO_2 Electroreduction from Carbonate Electrolyte. *ACS Energy Lett.* **4**, 1427–1431 (2019).

31. Luo, J. *et al.* Bipolar membrane-assisted solar water splitting in optimal pH. *Advanced Energy Materials* **6**, 1600100 (2016).

32. Na, J. *et al.* General technoeconomic analysis for electrochemical coproduction coupling carbon dioxide reduction with organic oxidation. *Nature Communications* **10**, 5193 (2019).

33. Han, X. *et al.* Electrocatalytic Oxidation of Glycerol to Formic Acid by $CuCo_2O_4$ Spinel Oxide Nanostructure Catalysts. *ACS Catal.* **10**, 6741–6752 (2020).

34. Li, T., Cao, Y., He, J. & Berlinguette, C. P. Electrolytic CO_2 Reduction in Tandem with Oxidative Organic Chemistry. *ACS Cent Sci* **3**, 778–783 (2017).

35. Verma, S., Lu, S. & Kenis, P. J. A. Co-electrolysis of CO_2 and glycerol as a pathway to carbon chemicals with improved technoeconomics due to low electricity consumption. *Nature Energy* **4**, 466 (2019).

36. Xia, C. *et al.* Continuous production of pure liquid fuel solutions via electrocatalytic CO_2 reduction using solid-electrolyte devices. *Nature Energy* **4**, 776–785 (2019).

37. Fan, L., Xia, C., Zhu, P., Lu, Y. & Wang, H. Electrochemical CO_2 reduction to high-concentration pure formic acid solutions in an all-solid-state reactor. *Nat. Commun.* **11**, 3633 (2020).

38. Salvatore, D. A. *et al.* Electrolysis of Gaseous CO_2 to CO in a Flow Cell with a Bipolar Membrane. *ACS Energy Lett.* **3**, 149–154 (2018).

39. Yan, Z., Hitt, J. L., Zeng, Z., Hickner, M. A. & Mallouk, T. E. Improving the efficiency of CO_2 electrolysis by using a bipolar membrane with a weak-acid cation exchange layer. *Nat. Chem.* **13**, 33–40 (2020).

40. Lee, D.-Y., Elgowainy, A. & Dai, Q. Life cycle greenhouse gas emissions of hydrogen fuel production from chlor-alkali processes in the United States. *Appl. Energy* **217**, 467–479 (2018).

41. Zhang, S. Prediction of selling price of hydrogen produced from methanol steam reforming. *Energy Sources*

Part B: Econ. Plan. Policy **13**, 28–32 (2018).

42. Kayfeci, M., Keçebaş, A. & Bayat, M. Hydrogen production. *Solar Hydrogen Production* 45–83 (2019) doi:10.1016/b978-0-12-814853-2.00003-5.

43. Shen, K.-Y., Park, S. & Kim, Y.-B. Hydrogen utilization enhancement of proton exchange membrane fuel cell with anode recirculation system through a purge strategy. *Int. J. Hydrogen Energy* **45**, 16773–16786 (2020).

44. Woo, C. H. & Benziger, J. B. PEM fuel cell current regulation by fuel feed control. *Chem. Eng. Sci.* **62**, 957–968 (2007).